frontiers | Frontiers in Nuclear Engineering

TYPE Original Research
PUBLISHED 16 November 2023
DOI 10.3389/fnuen.2023.1275396

OPEN ACCESS

EDITED BY
Alex Winkler,
University of Helsinki, Finland

REVIEWED BY
Shingo Tamaki,
Osaka University, Japan
Pawel Olko,
The Henryk Niewodniczański Institute of Nuclear Physics, Polish Academy of Sciences, Poland

*CORRESPONDENCE
M. E. Capoulat,
mcapoulat@gmail.com

RECEIVED 09 August 2023
ACCEPTED 23 October 2023
PUBLISHED 16 November 2023

CITATION
Capoulat ME and Kreiner AJ (2023), Induced radioactivity in AB-BNCT: an analysis of the different facilities worldwide.
Front. Nucl. Eng. 2:1275396.
doi: 10.3389/fnuen.2023.1275396

Induced radioactivity in AB-BNCT: an analysis of the different facilities worldwide

M. E. Capoulat[1,2,3]* and A. J. Kreiner[1,2,3]

[1]Department of Accelerator Technology and Applications, National Atomic Energy Commission (CNEA), Buenos Aires, Argentina, [2]National Scientific and Technical Research Council (CONICET), Buenos Aires, Argentina, [3]School of Science and Technology, National University of San Martín (UNSAM), Buenos Aires, Argentina

The global effort to establish Accelerator-Based Boron Neutron Capture Therapy (AB-BNCT) facilities involves various accelerator technologies and neutron-producing targets, each characterized by different properties of the primary beam and neutron spectra they generate. With an emphasis on long-term sustainability, it is essential to minimize the production of residual radioactivity to the lowest possible level, particularly given their intended use in a hospital environment. This paper aims to quantitatively assess the residual radioactivity in these facilities, taking into account both primary and secondary activation. Primary activation primarily arises from the interaction of the proton or deuteron beam and the neutron-producing target. Secondary activation results from neutron-induced reactions on the elements exposed to the neutron flux, with the Beam Shaping Assembly (BSA) being the most exposed one. To assess activation, we evaluated a representative group of target-BSA configurations. Primary activation was calculated based on cross-sectional data and the corresponding target materials. Neutron activation was assessed using Monte Carlo simulations with the MCNP 6.1 code. Regarding target activation, our findings indicate that ^{9}Be targets working with protons of less than 10 MeV represent the cleanest option, while ^{7}Li targets working with protons lead to the highest activation levels. As for BSA activation, the neutron energy is a crucial factor. In the case of standard BSA materials, higher neutron energy results in an increased number of potential reactions that produce radioactive products. Additionally, our findings suggest that radioactivity induced by impurities and minor components in alloyed materials cannot be disregarded and must be taken into account in radioactivity calculations. In summary, this research provides a comprehensive analysis of activation of the commonly used targets and BSA materials, aimed at contributing to the optimization of AB-BNCT facilities from a radiological perspective.

KEYWORDS

AB-BNCT, radioactivity, radiation protection, beam shaping assembly, neutron activation, neutron production targets

1 Introduction

Worldwide, several projects are underway to establish clinical facilities for Accelerator-Based Boron Neutron Capture Therapy (AB-BNCT). Some of these facilities are already operational and actively treating patients, and others are currently under development or/and in a construction stage. These projects are based on different accelerator technologies, neutron-producing reactions, and bombarding energies, as shown in Table 1.

TABLE 1 AB-BNCT facilities worldwide grouped by neutron producing reaction and beam energy.

Target-reaction	Beam energy (MeV)	Beam current goal (mA)	Institute, country	Refs
^{7}Li(p,n)^{7}Be	2.3–2.8	10–30	Xiamen Humanity Hosp., China	Aleynik et al. (2011), NEUBORON (2021), TAE Life Sciences (2021)
			IHEP, China	Chen et al. (2022)
			Helsinki Univ. Hospital, Finland	Neutron Therapeutics Inc (2019a), Neutron Therapeutics Inc (2019b), Porra et al. (2022)
			Soreq, Israel	Halfon et al. (2015)
			National Cancer Center, Japan	Nakamura et al. (2021), Matsumura et al. (2023)
			Edogawa Hospital, Japan	Nakamura et al. (2021), Matsumura et al. (2023)
			Nagoya University, Japan	Uritani et al. (2018), Watanabe et al. (2021)
			Shonan Kamakura Hospital, Japan	Neutron Therapeutics Inc (2019b), Neutron Therapeutics Inc (2023), Suzuki et al. (2023)
			Budker Inst., Russia	Aleynik et al. (2011)
			Granada University, Spain	Porras et al. (2020)
			Birmingham University, UK[a]	Neutron Therapeutics Inc (2019b), University of Birmingham (2022)
			CNAO, Italy	Aleynik et al. (2011), TAE Life Sciences (2021)
^{9}Be(p,n)^{9}B	30	1	Kyoto University, Japan	Tanaka et al. (2009), Mitsumoto et al. (2013)
			Kansai BNCT Res. Center, Japan	Tanaka et al. (2009), Kansai BNCT Medical Center (2019)
			Southern Tohoku Hosp., Japan	Tanaka et al. (2009), Kato et al. (2020), Southern Tohoku Hospital Group (2020)
^{9}Be(p,n)^{9}B	8	10	Tsukuba University, Japan	Kumada et al. (2014), Kumada et al. (2015), Kumada et al. (2019)
			Gachon Univ.-Dawon Medax, Korea	Lee et al. (2021a), Bae et al. (2022)
^{9}Be(d,n)^{10}B	1.45	30	CNEA, Argentina	Kreiner et al. (2007), Capoulat et al. (2014b), Cartelli et al. (2020)
^{13}C(d,n)^{14}N	1.45	30	CNEA, Argentina	Kreiner et al. (2007), Capoulat and Kreiner (2017), Cartelli et al. (2020)

[a]Not intended for clinical BNCT.

TABLE 2 Nuclear reactions and resulting radioactive products for different AB-BNCT targets.

	Product, $T_{1/2}$	Reaction	Threshold energy or Q-value (MeV)
^{7}Li + p	^{7}Be, 53.22 d	^{7}Li(p,n)^{7}Be	E_{thres} = 1.88
^{9}Be + p	^{7}Be, 53.22 d and tritium, 12.32 y	^{9}Be(p,t)^{7}Be	E_{thres} = 13.432
		^{9}Be(p,d + *n*)^{7}Be	E_{thres} = 20.4
		^{9}Be(p,p+2n)^{7}Be	E_{thres} = 22.9
^{9}Be + d	tritium, 12.32 years	^{9}Be(d,t)^{8}Be	Q = 4.602
^{13}C + d	tritium, 12.32 years	^{13}C(d,t)^{12}C	Q = 1.312
	^{14}C, 5,700 years	^{13}C(d,p)^{14}C	Q = 5.962

Among these, there are high-energy 30 MeV cyclotrons that utilize the ^{9}Be(p,n) reaction, as well as medium-energy RFQ-DTL accelerators operating at 8 and 10 MeV also employing the ^{9}Be(p,n) reaction. Additionally, there are low-energy electrostatic accelerators (both Tandem and Single-Ended) and RFQ machines that work with ^{7}Li(p,n) at around 2.5 MeV, and a very low-energy electrostatic quadrupole ESQ accelerator operating with the ^{9}Be(d,n) or ^{13}C(d,n) reactions at 1.45 MeV. A more comprehensive compilation is provided in (Matsumura et al., 2023) (exclusively for projects in Japan) and in "Advances in BNCT"

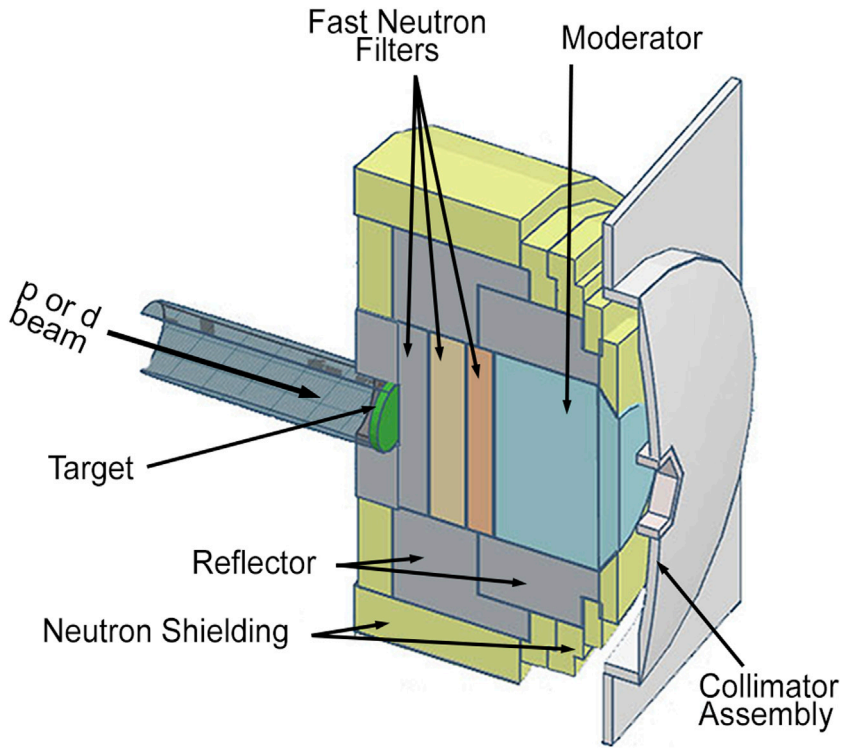

FIGURE 1
Schematic view of a typical Beam Shaping Assembly (BSA). Extracted from (Capoulat and Kreiner, 2022).

(International Atomic Energy Agency, 2022) which covers global projects.

Considering that these facilities are intended to operate within hospitals, an essential guiding principle should be the ALARA (As Low As Reasonably Achievable) criterion. With a focus on long-term sustainability, it is crucial to limit the production of residual radioactivity to the lowest possible level, following the ALARA criterion.

The purpose of this study is to quantitatively assess the residual radioactivity in AB-BNCT facilities, considering both primary and secondary activation.

Primary activation occurs due to the interaction of the proton or deuteron beam with various subsystems of the accelerator, resulting in nuclear reactions (p,X) or (d,X), where X represents any open reaction channel leading to radioactive products. The radioactive product can be either the ejected particle or the heavy product of the reaction. The most critical subsystem concerning primary activation is the target material, since the major part of the beam directly impacts it. Table 2 summarizes the radioactive products and nuclear reactions relevant to each type of projectile and target material.

Secondary activation is a result of neutron-induced reactions (n,X) occurring in any element exposed to the neutron flux. Numerous subsystems can be activated, including the BSA, shielding, target assembly, irradiation room walls, beamline, ancillary equipment, wires, and other elements exposed to neutrons. Among these subsystems, the BSA holds particular significance, as it is located in close proximity to the neutron-producing target. Its primary function is to moderate the neutrons to the epithermal regime and efficiently guide them towards the element intended for irradiation, effectively filtering out fast and thermal neutrons as well as gamma rays. Due to its close proximity to the neutron-producing target, the BSA is the most exposed subsystem, making it susceptible to significant activation. Figure 1 shows a layout of a BSA indicating the constituent elements.

2 Materials and methods

2.1 Activity calculation

Daily operations typically involve alternating periods of continuous irradiation and downtime. During irradiation, the activity, denoted A, accumulates according to the following equation:

$$A(t) = \left(A_0 - \frac{p}{\lambda}\right)\cdot e^{-\lambda\cdot t} + \frac{p}{\lambda} \tag{1}$$

In Eq. 1, t is the irradiation time, p is the activity production rate, λ is the decay constant of the radioactive residue and A_0 is the activity at the beginning of the irradiation.

During downtime, the activity follows the radioactive decay law:

$$A\left(t + t'\right) = A(t)\cdot e^{-\lambda\cdot t'} \tag{2}$$

Here, t' denotes the length of downtime.

For a given scheme of operation, the activity accumulated over time can be computed by alternately applying (Eqs 1, 2). Consider a daily scheme of 8 h of irradiation followed by 16 h of downtime (i.e., $t = 8\,h$ and $t' = 16\,h$). The activity immediately after irradiation on the N^{th} day of operation, $A(N)$, can be expressed as:

$$A(N) = \left[A(N-1)\cdot e^{-\lambda\cdot 16\,h} - \frac{p}{\lambda}\right]\cdot e^{-\lambda\cdot 8\,h} + \frac{p}{\lambda} \quad (3)$$

Or equivalently,

$$A(N) = A(N-1)\cdot e^{-\lambda\cdot 24h} + \frac{p}{\lambda}\left(1 - e^{-\lambda\cdot 8\,h}\right) \quad (4)$$

Following this recurrence, $A(N)$ can be written in terms of the activity accumulated over the first day of operation, $A(1)$:

$$A(N) = A(1)\cdot\left(e^{-\lambda\cdot 24h}\right)^{N-1} + \frac{p}{\lambda}\left(1 - e^{-\lambda\cdot 8\,h}\right)\cdot\sum_{k=0}^{N-2}\left(e^{-\lambda\cdot 24h}\right)^{k} \quad (5)$$

We can obtain $A(1)$ from Eq. 1 by setting $A_0 = 0$, since the activity at the beginning of the first day of operation is zero. Therefore, $A(N)$ can be expressed as:

$$A(N) = \frac{p}{\lambda}\left(1 - e^{-\lambda\cdot 8\,h}\right)\cdot\sum_{k=0}^{N-1}\left(e^{-\lambda\cdot 24h}\right)^{k} \quad (6)$$

The sum in Eq. 6 is the geometric series $\sum_{k=0}^{N-1} r^k$ with $r = e^{-\lambda\cdot 24\,h}$. When $|r| < 1$ (as is the case here), the sum is calculated as $\frac{1-r^N}{1-r}$. Thus, for the considered scheme of operation (8 h of irradiation followed by 16 h of downtime), the activity immediately after irradiation on the N^{th} day of operation can be calculated as:

$$A(N) = \frac{p}{\lambda}\cdot\left(1 - e^{-\lambda\cdot 8\,h}\right)\cdot\frac{1 - \left(e^{-\lambda\cdot 24\,h}\right)^{N}}{1 - e^{-\lambda\cdot 24\,h}} \quad (7)$$

2.2 Target activation

For the targets, the activity production rate (p) was calculated from reaction cross-sections $\sigma(E)$ as:

$$p = \lambda\cdot\dot{n}\cdot n_A\int S(E)^{-1}\cdot\sigma(E)\cdot dE \quad (8)$$

Where $\dot{n}$ (in 1/s) is the number of projectiles (protons or deuterons) per second impinging on the target, n_A is the atom density of the target, $S(E)$ is the stopping power. Cross-sections were taken from (Hermanne et al., 2014; Koning et al., 2019; Nakayama et al., 2021; National Nuclear Data Center, 2022) and stopping powers from (Ziegler et al., 2010).

2.3 Beam shaping assembly activation (BSA)

In the initial stage, we conducted a comprehensive analysis of the activation generated in commonly used BSA materials. Our primary goal was to identify the most significant neutron-induced reactions leading to radioactivity in each material. Considering that reaction cross-sections depend on neutron energy, we organized our analysis into three categories: low (up to ~1 MeV), intermediate (up to ~8 MeV), and high-energy (up to ~28 MeV). Secondly, we specifically analyzed some representative BSAs for each group. Using information gathered from publications by various AB-BNCT facilities worldwide, we set up and simulated each BSA with the MNCP 6.1 code (Goorley et al., 2012).

The low-energy group includes the facilities using 2.1–2.8 MeV protons on lithium targets, where the maximum energy of the neutron spectrum is of the order of 1 MeV or less, depending on the proton energy. Specifically, for protons of 2.3 MeV, the maximum neutron energy is 573 keV. This group of facilities report using moderators of MgF_2 (Uritani et al., 2018; Li et al., 2021; Torres-Sánchez et al., 2021; Qiao et al., 2023), AlF_3 (Lee et al., 2021), CaF_2 (Wang et al., 2022) and Fluental™ (Chen et al., 2021). As representative cases, we analysed the case of 2.3 protons with all the aforementioned moderators.

The intermediate-energy group includes facilities that produce neutrons up to about 8 MeV. Within this category, we find those using ^{13}C and ^{9}Be targets with deuterons of 1.45 MeV, as well as facilities utilizing ^{9}Be targets with protons of 8–10 MeV. Their maximum neutron energies are 6.72, 5.76, and 6.13–8.14 MeV, respectively. Facilities employing 8–10 MeV protons on beryllium targets have reported the use of MgF_2 moderators in conjunction with a fast neutron filter of iron (Kumada et al., 2018; Kumada et al., 2019; Bae et al., 2022). Meanwhile, facilities employing 1.45 MeV deuterons on ^{13}C and ^{9}Be targets use alternating slabs of Al and PTFE (Al + PTFE) as moderators (Capoulat and Kreiner, 2017) and AlF_3 moderators (Capoulat, 2014a; Capoulat et al., 2014b). As representative cases within this group, we analyzed the scenario involving 8 MeV protons on a beryllium target and the scenario of 1.45 MeV deuterons on both ^{13}C and ^{9}Be targets, all of them utilizing their respective BSAs.

Lastly, the high-energy group includes facilities employing ^{9}Be targets with 30 MeV protons. These facilities produce neutrons with energies up to of 28.15 MeV. Moderators of CaF_2 with filters of aluminium, iron and lead are reported for this group (Mitsumoto, 2023), and considered here as a representative case.

Table 3 summarizes the configurations considered here, including their main elements such as the moderator, fast neutron filters, and reflector. It is pertinent to remind that this study exclusively focuses on the aspect of radioactivity generation. Assessing the neutron beam quality achievable with each analyzed configuration falls outside the scope of our research. For details on this issue, refer to the citations in Table 3.

To assess secondary activation, energetically allowed neutron-induced nuclear reactions with up to 4 light products were considered for each element. For a nuclear reaction with cross-section σ, the activity production rate p is:

$$p = \lambda\cdot N_A\int\dot{\phi}(E)\cdot\sigma(E)\cdot dE \quad (9)$$

where $\dot{\phi}(E)\cdot dE$ (in 1/cm^2-s) is the neutron flux in the element to evaluate (moderator, fast neutron filters or reflector), N_A is the number of target atoms for the reaction that generates radioactivity in the element of interest. The integrals in Eq. 9 were calculated as F4 Tallies with the reaction cross-sections as the tally modifiers (DE and DF cards). Cross-sections were taken from different evaluated databases (Sublet et al., 2010; Brown et al., 2018; Koning et al., 2019).

The accumulated activity concentration of each radioactive product was calculated as indicated in Eq. 7 and compared to the levels of clearance given in the IAEA Safety Guide RS-G1.7 (International Atomic Energy Agency, 2004). The clearance levels represent the maximum activity concentration tolerable to release radioactive materials from regulatory control. The values are derived for each radionuclide in the IAEA Safety Report No44 (International Atomic Energy Agency, 2005), and correspond to the activity

TABLE 3 Description of the beam shaping assemblies considered in this study.

	Beam energy, current	Moderator	Fast neutron filter	Reflector	Refs
^{7}Li + p	2.3 MeV, 30 mA	Fluental™, MgF_2, AlF_3 or CaF_2	None	Pb	Chen et al. (2021)
					Li et al. (2021)
					Uritani et al. (2018)
					Torres-Sánchez et al. (2021)
					Qiao et al. (2023)
					Lee et al. (2021b)
					Wang et al. (2022)
^{9}Be + p	8.0 MeV, 10 mA	MgF_2	Fe	Pb	Kumada et al. (2018)
					Bae et al. (2022)
^{9}Be + p	30 MeV, 1 mA	CaF_2	3: Pb + Fe + Al	Pb	Tanaka et al. (2011)
					Mitsumoto (2023)
^{9}Be + d	1.45 MeV, 30 mA	PTFE + Al or AlF_3	None	Pb	Capoulat et al. (2014b)
					Capoulat (2014a)
^{13}C + d	1.45 MeV, 30 mA	PTFE + Al or AlF_3	None	Pb	Capoulat and Kreiner (2017)
					Capoulat (2014a)

concentration values such that individual effective doses to a critical group (i.e., the public and workers) would be of the order of 10 μSv/a and would have only a very low probability of approaching an individual dose of 1 mSv/a.

For materials containing a mixture of radionuclides, the normalized activity concentration (C) is defined as:

$$C = \sum_{i=1}^{n} \frac{C_i}{L_i} \quad (10)$$

where C_i is the concentration (in Bq/g) of the ith radionuclide in the material, L_i is the respective activity concentration for clearance and n is the number of radionuclides present (ref paragraph 4.7 in the RS-G1.7 Safety Guide).

Materials containing radioactivity can be cleared if C < 1 and $Ci < L_i$ for all radionuclides present in the material. If these conditions are not met, the cooling time is estimated as the decay time required to meet the clearance condition after retirement from service.

3 Results

3.1 Target activation

The ^{9}Be + p case, using 8 MeV protons, represents the cleanest target. In this scenario, all reaction channels leading to radioactivity are energetically forbidden (refer to Table 2). Only short-lived light radionuclides, such as ^{9}Be(p,n)^{9}B (with a threshold energy of 2.057 MeV), ^{9}Be(p,d)^{8}Be (with a Q value of 570 keV), and ^{9}Be(p,p + n)^{8}Be (with an energy threshold of 1.850 MeV) are produced. The resulting products are ^{9}B (with an energy width of 0.54 keV) which decays *via* proton emission to ^{8}Be, and ^{8}Be which rapidly disintegrates into two alpha particles without emitting gamma radiation.

All the other targets produce activation, as depicted in Figure 2. The total activity accumulated during the initial 30 days of operation is plotted for each target. Among them, the lithium target (Li + p) exhibited the highest activity, resulting from the radioactive isotope ^{7}Be (with a half-life of 53.22 days) generated by the neutron-producing reaction ^{7}Li(p,n)^{7}Be. This radionuclide undergoes electron capture, emitting a 478 keV gamma ray in 10.44% of the decays (yielding ^{7}Li as a product). After 30 days of operation, 2.1 TBq of ^{7}Be accumulate on the target, with nearly 82 GBq accumulating within the first day.

Next in importance is the beryllium target bombarded with 30 MeV protons (^{9}Be + p(30 MeV)). The activity of ^{7}Be amounts to 390 GBq during 30 days of operation and 15 GBq within the first day. This activity results from various reactions, including ^{9}Be(p,t), ^{9}Be(n,d + n), and ^{9}Be(n,p+2n). Additionally, the ^{9}Be(p,t)^{7}Be reaction produces tritium (4.2 GBq in 30 days). This radionuclide emits very low-energy beta particles (E < 18.591 keV), and it does not emit any gamma rays. Due to its long half-life (12.32 years), tritium accumulates at a slower rate compared to ^{7}Be, hence, for short periods of time, the activity in this target is primarily attributed to ^{7}Be.

When utilizing deuterons on beryllium and ^{13}C targets (^{9}Be + d and ^{13}C + p), only low-energy pure beta emitters are produced. In the case of the beryllium target, 4.1 GBq of tritium are generated through the ^{9}Be(d,t) reaction during an 30-day period, with 150 MBq produced within the first day. Concerning the ^{13}C target, it primarily results in the generation of tritium, with a small amount of ^{14}C. This radionuclide emits low energy beta particles up to 156 keV. Compared to other options, the production of tritium with this target is significantly lower (780 MBq over 30 days, 2.7 MBq within the first day).

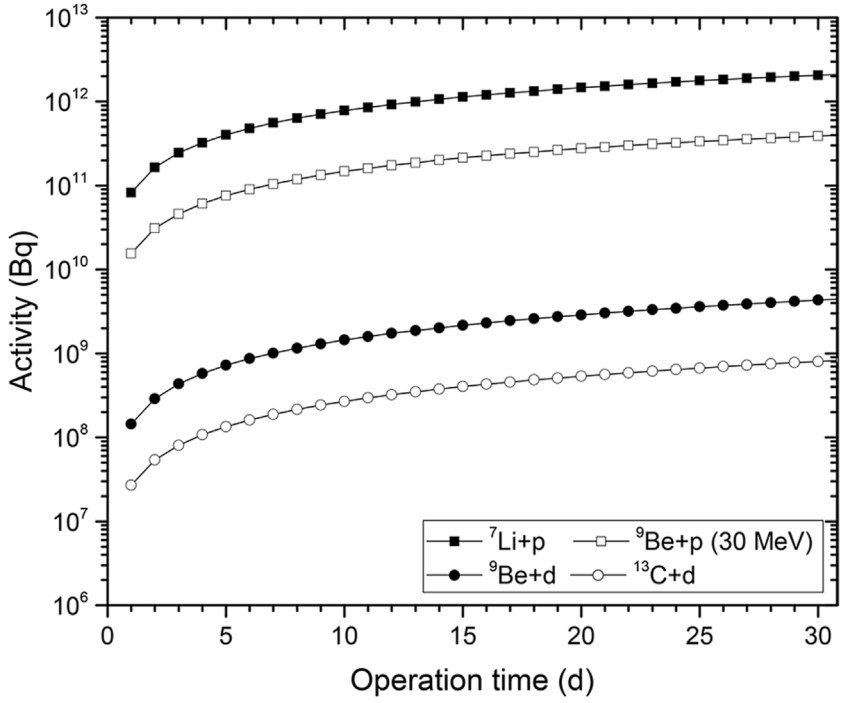

FIGURE 2
Total activity accumulated in different targets.

3.2 Beam shaping assembly (BSA) activation

Table 4 presents a compilation of the most relevant radionuclides generated through neutron activation in commonly used materials for low, intermediate, and high-energy facilities. The materials are grouped according to their roles in the BSA, namely, moderator, reflector, fast neutron filter, and fast neutron shielding. Only radionuclides that exceed the clearance level after 5 years of operation are shown. Radionuclides in each group are sorted in decreasing order of relevance concerning the determination of cooling time. Short-lived radionuclides ($T_{1/2}$ < 2 h) are not included, as they have no significant impact on the cooling time. The following subsection discusses each group of materials in detail.

3.2.1 Moderator materials

Moderator materials referred to in the literature for producing epithermal neutron beams include calcium (CaF_2) and magnesium (MgF) fluorides, Fluental™ (AlF_3: 69 wt%, metallic aluminum: 30 wt %, and LiF: 1 wt%), AlF_3 and aluminum (Al).

In pure aluminum, long-term activation occurs exclusively in the high-energy facilities. Tritium ($T_{1/2}$ = 12.32 years) and ^{22}Na ($T_{1/2}$ = 2.6018 years) are produced through the ^{27}Al(n,t) and the ^{27}Al(n, 2n+α) reactions, respectively. These reactions have threshold energies of 11.29 and 23.35 MeV, resulting in the complete absence of long-term radioactivity accumulation in the low and intermediate energy groups. ^{24}Na ($T_{1/2}$ = 14.997 h) is produced mainly by the ^{27}Al(n,α)^{24}Na reaction, with a threshold energy of 3.25 MeV in intermediate and high-energy facilities.

It is worth mentioning that pure aluminum is not used for structural applications due to its limited strength, corrosion resistance, and lack of other desirable properties for that purpose. In commercially available aluminum alloys, metals or semimetals (such as Si, Fe, Cu, Mn, Mg, Zn, and others) are added to aluminum to enhance its structural properties. The presence of these minor components must also be considered when analyzing neutron activation.

In the 1,050 Al alloy (≥99.5 wt% Al, <0.25 wt% Si, <0.4 wt% Fe, <0.05 wt% Mg, <0.05 wt% Mn, <0.05 wt% Zn, <0.05 wt% V, and <0.03 wt% Ti), neutron activation leads, among others, to the accumulation of ^{65}Zn ($T_{1/2}$ = 243.93 d), ^{54}Mn ($T_{1/2}$ = 312.2 d) and ^{59}Fe ($T_{1/2}$ = 44.495 d). These radionuclides result from the activation of the alloying Zn and Fe exclusively. Simulations made for intermediate-energy facilities showed that these radionuclides can extend the cooling time to several years (whereas pure aluminum cools down within a few days).

Fluental™, also employed as a moderator, accumulates tritium ($T_{1/2}$ = 12.32 years) resulting from the ^{6}Li(n,α)^{3}H reaction. This exothermic reaction (Q = 4.783 MeV) is relevant for all energy groups. In the intermediate and high-energy groups, the accumulation of ^{24}Na ($T_{1/2}$ = 14.997 h) is also observed, arising from the ^{27}Al(n,α)^{24}Na reaction. Moreover, in the high-energy group, as more reaction channels become accessible, additional radionuclides are generated, including ^{18}F ($T_{1/2}$ = 109.77 min, not shown in Table 4) and ^{22}Na ($T_{1/2}$ = 2.6018 years). Among these, only the last one is relevant for long-term accumulation and may have some additional impact on the cooling time.

In pure calcium fluoride (CaF_2), several exothermic and low-threshold energy reactions on natural calcium result in the formation of radioactive isotopes of Ca and K, impacting the radioactivity production in all energy groups. As far as long-term

TABLE 4 Key radionuclides generated through neutron activation in some BSA materials for low, intermediate, and high-energy facilities. Radionuclides are sorted by cooling time relevance. Short-lived radionuclides ($T_{1/2}$ < 2 h) are excluded.

Neutron-energy group	Low	Intermediate	High	
Moderator Materials:	Aluminium (pure)	-	^{24}Na	^{3}H, ^{22}Na, ^{24}Na
	Aluminium Alloy (1050)	^{65}Zn, ^{54}Mn, ^{59}Fe, ^{56}Mn and ^{64}Cu	^{65}Zn, ^{54}Mn, ^{59}Fe, ^{46}Sc, ^{56}Mn, ^{24}Na and ^{64}Cu	^{3}H, ^{60}Co, ^{65}Zn, ^{22}Na, ^{54}Mn, ^{55}Fe, ^{47}Ca, ^{59}Fe, ^{24}Na, ^{48}Sc, ^{64}Cu, ^{56}Mn and ^{69}Zn
	Fluental™	^{3}H	^{3}H and ^{24}Na	^{3}H, ^{24}Na and ^{22}Na
	MgF_2 (pure)		^{24}Na	^{3}H, ^{22}Na, ^{24}Na and ^{14}C‡
	CaF_2 (pure)	^{45}Ca and ^{47}Ca	^{45}Ca and ^{47}Ca	^{3}H, ^{45}Ca, ^{47}Ca, ^{43}K, ^{42}K and ^{14}C‡
	AlF_3 (pure)	-	^{24}Na	^{3}H, ^{22}Na, ^{24}Na and ^{14}C‡
Reflector Materials:	Lead (pure)	-	-	^{204}Tl, ^{203}Hg and ^{203}Pb
Fast Neutron Filter Materials:	Iron (pure)	^{55}Fe, ^{54}Mn, ^{59}Fe, ^{51}Cr and ^{56}Mn	^{55}Fe, ^{54}Mn, ^{59}Fe, ^{51}Cr and ^{56}Mn	^{3}H, ^{55}Fe, ^{54}Mn, ^{59}Fe, ^{51}Cr, ^{52}Mn and ^{56}Mn
	Iron alloy	^{55}Fe, ^{54}Mn, ^{59}Fe and ^{51}Cr	^{55}Fe, ^{54}Mn, ^{59}Fe, ^{51}Cr, ^{32}P, ^{56}Mn and ^{31}Si	^{3}H, ^{55}Fe, ^{54}Mn, ^{59}Fe, ^{51}Cr, ^{52}Mn, ^{32}P, ^{24}Na, ^{56}Mn and ^{31}Si
	Lead (pure)	-	-	^{204}Tl, ^{203}Hg and ^{203}Pb
Fast Neutron Shielding Materials:	Lithiated polyethylene	^{3}H	^{3}H and ^{24}Na‡‡	^{3}H, ^{24}Na‡‡ and ^{14}C‡‡‡
	Boronated Paraffin (pure ‡‡‡‡)	^{3}H‡	^{3}H‡	^{3}H

‡The accumulation of this radionuclide becomes relevant only after more than 15 years of operation.
‡‡Only SWX™-215 Litihiated polyethylene (7.5%w ^{nat}Li).
‡‡‡Only in 50%-w LiF loaded polyethylene, only after 15 years of operation.
‡‡‡‡Due to the potential impurities in paraffin, other omitted radionuclides may also relevant.

activation is concerned, the most relevant one is ^{45}Ca ($T_{1/2}$ = 162.61 days), followed by ^{47}Ca ($T_{1/2}$ = 4.536 days) for the low and intermediate-energy groups. In the high-energy group, tritium-producing reactions (n,t) are energetically allowed, making tritium the most significant product for determining the cooling period. Additionally in this group, ^{43}K ($T_{1/2}$ = 22.3 h) and ^{42}K ($T_{1/2}$ = 12.355 h) and ^{18}F ($T_{1/2}$ = 109.77 min, not shown in Table 4) are without significant impact on the cooling time. For longer periods of operation (10–15 years or more), a non-negligible activity ^{14}C will be present due to the ^{19}F(n, d+ α). Given its long half-life, the clearance time is significantly prolonged once this radionuclide exceeds its clearance level. Hence, to limit the cooling time of the material, it is crucial to limit the operation time in order to maintain the activity concentration of ^{14}C below the clearance level.

In pure magnesium fluoride (MgF_2) and aluminum fluoride (AlF_3), no long-term activation is generated in the low-energy group of facilities. Within this group, the only energetically allowed reactions are ^{19}F(n,γ)^{20}F (present in both MgF_2 and AlF_3), ^{26}Mg(n,γ)^{27}Mg (in MgF_2) and ^{27}Al(n,γ)^{28}Al (in AlF_3), all of which are exothermic processes. Due to their short half-lives (11.07 s for ^{20}F and 9.458 min for ^{27}Mg), these radionuclides do not accumulate in MgF_2. Similarly, in pure AlF_3 where ^{20}F and ^{28}Al ($T_{1/2}$ = 2.246 min) are present, no radioactivity accumulates. Within intermediate-energy facilities, only ^{24}Na ($T_{1/2}$ = 14.997 h) is produced. In MgF_2, it forms through the endothermic ^{24}Mg(n,p) reaction, with a threshold energy of 4.932 MeV. In AlF_3, ^{24}Na is produced through the endothermic ^{27}Al(n,α)^{24}Na reaction, with a threshold energy of 3.25 MeV. This may result in some radioactivity accumulation in the long-term operation of both MgF_2 and AlF_3 moderators. However, considering the half-life of ^{24}Na, the cooling time is not expected to be excessively long. In high-energy facilities, other reaction channels leading to long-lived radionuclides become energetically accessible. Among these, ^{3}H ($T_{1/2}$ = 12.32 years) and ^{22}Na ($T_{1/2}$ = 2.6018 years) are the most relevant ones both in and AlF_3. As in the CaF_2 moderator, some activity of ^{14}C ($T_{1/2}$ = 5,700 years) may be non-negligible for longer times of operation.

3.2.2 Reflector

Most reflectors referred to in the literature are made of lead (Pb). In pure lead, several exothermic reactions lead to the production of radioactive isotopes. The highest activity is attributed to ^{209}Pb ($T_{1/2}$ = 3.324 h) generated through the radiative capture (n,γ) reaction on ^{208}Pb. The IAEA Safety Guide RS-G1.7 does not specify a clearance level for this particular radioisotope. Therefore, it was omitted from Table 4, and its contribution was not considered for estimating the cooling time. This radionuclide exclusively emits beta particles (no γ) with energies up to 197.5 keV, and nearly all Bremsstrahlung radiation resulting from the deceleration of beta particles is self-absorbed in the reflector, except for a small fraction originating from ^{209}Pb in the outer shell of lead. Hence, this activity is expected to have a minor impact on radiation exposure.

Other radioactive products from exothermic reactions are ^{197}Pt ($T_{1/2}$ = 19.8915 h), ^{200}Pt ($T_{1/2}$ = 12.6 h), ^{203}Hg ($T_{1/2}$ = 46.567 days) and ^{204}Tl ($T_{1/2}$ = 3.783 years). For low and intermediate-energy facilities, the activities from these radionuclides were found to not exceed the clearance level after several years of operation, when lead is used as a reflector.

Concerning high-energy facilities, the activities of ^{204}T, ^{203}Hg, and also ^{203}Pb ($T_{1/2}$ = 51.92 h) are the most relevant products to determine the cooling time. Simulations showed that tritium resulting from (*n*,*t*) nuclear reactions on lead will not be significant for up to several decades of operation.

It is worth mentioning that commercial high-purity lead in bulk often contains small amounts of other elements, such as cadmium (Cd), bismuth (Bi), tin (Sn), antimony (Sb), copper (Cu), and arsenic (As). These elements are added to the alloy to enhance the physical and mechanical properties of pure lead. When analyzing neutron activation, it is essential to consider these minor components. From these, the most significant radioactive products are ^{122}Sb ($T_{1/2}$ = 2.7238 days) and ^{76}As ($T_{1/2}$ = 1.0942 days), resulting from the radiative capture (*n*,*γ*) reactions on antimony and arsenic, respectively. Simulations showed that these activities will reach the clearance levels in less than only 1 year of service of the reflector, even for small amounts of arsenic and antimony (0.0001 and 0.002 wt%, respectively). For low and intermediate-energy facilities, these components are indeed the ones that determine the cooling time, considering that the only product generated in pure lead ^{209}Pb has a shorter half-life.

3.2.3 Fast neutron filters

In this study, the term "fast neutron filter" refers to the initial layer or layers of materials adjacent to the target and situated before the moderator. Iron (Fe) is utilized in certain intermediate-energy facilities. In high-energy facilities, layers of lead, iron, and aluminum are employed simultaneously (refer to Table 3).

In pure iron, several exothermic and low-threshold energy reactions contribute to the accumulation of radioactivity. The primary contributor to this activity is ^{56}Mn (with a half-life of 2.58 h), which is generated in the ^{56}Fe(n,p) reaction. However, when considering long-term generation of residues, ^{55}Fe and ^{54}Mn (generated through ^{54}Fe(*n*,*γ*) and ^{54}Fe(*n*,*p*), respectively) become more relevant to determine the cooling time of the filter due to their longer half-lives (2.744 years and 312.2 days, respectively). Simulations showed that for intermediate and high-energy facilities the cooling times of these filters are of the order of 20 years, after 5 years of operation.

Commercial iron contains small amounts of alloying elements, including carbon (C), silicon (Si), manganese (Mn), sulfur (S), and phosphorus (P), to enhance the mechanical and chemical properties of the iron. Simulations showed that the presence of these elements slightly increases the activity of ^{56}Mn (resulting from radiative capture on ^{55}Mn) and generates additional radioactivity of ^{24}Na ($T_{1/2}$ = 14.997 h), ^{31}Si ($T_{1/2}$ = 157.36 m), ^{32}P ($T_{1/2}$ = 14.268 days). However, their influence on the cooling time is expected to be minimal when compared to that obtained for a pure iron filter.

Concerning lead filters (used in the high-energy facilities) the isotopes ^{203}Pb ($T_{1/2}$ = 51.92 h), ^{203}Hg ($T_{1/2}$ = 46.567 days) and ^{204}Tl ($T_{1/2}$ = 3.783 years) are the main radioactive products as similarly observed in the lead reflector. Due to the proximity to the target, the filter is exposed to a much higher neutron flux as compared to the reflector. Consequently, the activities and, therefore, the cooling times are larger. Simulations showed that nearly 38 years of cooling would be required after just 1 year of service for the filter.

In pure aluminum filters, the relevant radionuclides concerning long-term radioactivity are the same as those mentioned above for aluminum moderators. Similarly, for aluminum alloys, the radioactivity produced by the activation of alloying elements must be considered, even for high-aluminum content alloys.

3.2.4 Fast neutron shielding

Lithiated polyethylene and boronated paraffin are common materials for fast neutron shielding (and also thermal neutron shielding). Most of the commercial lithiated polyethylene contains 7.5 wt% of natural Li[1,2]. Other polyethylenes containing 50 wt% of lithium fluoride (LiF) are also used (Komori et al., 2023).

In lithium polyethylene, tritium ($T_{1/2}$ = 12.32 years), primarily generated in the exothermic ^{6}Li(n,α)^{3}H reaction, is produced in the long term. Light elements such as carbon, oxygen, and hydrogen present in polyethylene mainly produce very short-lived light residues, with half-lives ranging from milliseconds to seconds. The activity of ^{14}C ($T_{1/2}$ = 5,700 years), coming from the exothermic (n,γ) reaction on ^{13}C is expected to be low due to the small abundance of ^{13}C in natural carbon (1.07%). Simulations made for intermediate-energy facilities demonstrate that the concentration activity of ^{14}C remains below the clearance level even after several decades of operation.

Some commercial lithium polyethylene may contain impurities such as chlorine (Cl), calcium (Ca), and sodium (Na), typically in the range of 0.001–0.004 wt% each. Simulations for intermediate-energy facilities showed that the activity of ^{24}Na ($T_{1/2}$ = 14.922 days) exceed the clearance level in less than 1 year of operation. However, due to its much shorter half-life compared to tritium, it does not significantly impact cooling times.

In lithium polyethylene containing LiF, when used in high-energy facilities, also ^{18}F coming from the endothermic (E_{thres} = 10.432 MeV) ^{19}F(n, 2n) reaction rapidly accumulates after a few hours of operation. However, due to its short half-life ($T_{1/2}$ = 109.77 min), it rapidly decays, having no impact on long-term accumulation. Some activity of ^{14}C ($T_{1/2}$ = 5,700 years) is expected due to the ^{19}F(n, d+ *α*), which may have an impact on the cooling time if the ^{14}C clearance level is exceeded.

In pure paraffin loaded with 66% wt of pure boric acid, only some activity of tritium is generated in the long-term operation through the exothermic ^{10}B(n, 2α)^{3}H reaction. Simulations for intermediate-energy facilities showed that the accumulated activity remains below the tritium's clearance level even after several decades of irradiation. Obtaining pure paraffin, however, is difficult, and additionally, the type and level of impurities vary greatly depending on its origin and manufacturing process. X-Ray Fluorescence (XRF) analysis conducted for different samples in our laboratory revealed small but non-negligible amounts of Ca (9.6 wt %), Cl (0.13 wt%), Fe (0.17 wt%), Cu (0.0012 wt%), Ni (0.001 wt%), Zn (0.0002 wt%) among others. Additionally, trace amounts of heavy metals (Pb, Hg, and Cd) were also detected. Considering these elements, simulations were conducted for intermediate-energy facilities using a boronated paraffin shielding surrounding the reflector. It was found that, only ^{65}Zn ($T_{1/2}$ = 243.93 days,

1 Shieldwerx SWX-215 Poly-based Shielding. https://www.shieldwerx.com/poly-based-shielding. Accessed 7 August 2023.

2 JCS Nuclear Solutions JC215 Lithium Polyethylene. https://johncaunt.com/products/lithium-polyethylene/. Accessed 7 August 2023.

produced in the radiative capture on ^{64}Zn) resulted in long-term accumulation. All other radioactive residues remained below their respective clearance levels even after several decades of service. However, considering the variety of potential impurities in this material, each case must be analyzed carefully.

3.3 Evaluation of a representative group of beam

3.3.1 ^{7}Li + p (2.3 MeV)

Only Fluental and CaF_2 moderators become activated. Moderators composed of pure AlF_3 and pure MgF_2 does not produce long-term radioactivity, as described in §3.2.1. Figure 3 shows the normalized concentration activity (C) as a function of the operation time, with the corresponding cooling times indicated as dot labels for a Fluental and a CaF_2 moderator. In Fluental, C is due to tritium, and in CaF_2 it is due to ^{45}Ca with a small contribution of ^{47}Ca.

In the lead reflector, none of the products individually or together exceed the clearance level, regardless of the moderator material.

3.3.2 ^{9}Be + d (1.45 MeV) and ^{13}C + d (1.45 MeV)

Both in the PTFE + Al and AlF_3 moderators, the element of concern is aluminum. Activation of PTFE in the PTFE + Al moderator remains negligible even in a long-term operation, as the saturation activities of all radioactive products, as well as their normalized sum, remain well below the clearance levels. Fluorine in AlF_3 produces only very short-lived ^{20}F ($T_{1/2}$ = 11.07 s). Figure 4 illustrates the values of C for these moderators over the operational period. Both pure aluminum and the 1,050 alloy are considered for the aluminum present in the PTFE + Al moderator.

Pure aluminum generates ^{24}Na as the sole radioactive product, with a half-life of 14.922 days. This radionuclide decays to slightly less than half its initial concentration during a 16-h daily downtime. After about 4 days of operation, an effective saturation level is reached, and upon retiring the material from service, it requires a cooling time of 4.2 days. In the 1,050 alloy, C values and cooling times are substantially larger, attributed to the activation of its alloying elements. The cooling process is mainly determined by two key nuclides: ^{65}Zn (with a half-life of 243.93 days) and ^{54}Mn (with a half-life of 312.2 days), which are produced by the activation of natural Zn and Mn, respectively.

In the pure AlF_3 moderator no long-term radioactivity is produced, as described in §3.2.1. The 3.2-day cooling time shown in Figure 4 is due to ^{24}Na resulting from the activation of aluminum.

As for the lead reflector, the saturation activities of all radioactive products, along with their normalized sum, consistently stay well below the allowable levels, whether using an AlF_3 or PTFE + Al moderator. Consequently, the values of C will remain below 1 throughout the reflector's operational lifespan.

3.3.3 ^{9}Be + p (8 MeV)

Figure 5 illustrates the C values and cooling times throughout the operation time for both a pure iron and an iron alloy fast neutron filter. In the pure material, the most important contribution to the C value arises from ^{54}Mn (with a half-life of $T_{1/2}$ = 312.2 days) over the entire range of operation time. In the alloy, in addition, there is an even more substantial contribution of ^{56}Mn resulting from the activation of alloying natural manganese, which significantly increases the C value during the first year of service. Due its short half-life ($T_{1/2}$ = 2.5789 h), the presence of ^{56}Mn has no impact on the cooling times when compared to the pure material, where natural manganese is absent, both for pure iron and the alloy. In both materials, cooling times are determined by ^{54}Mn until it reaches the saturation level at about 3 years of service, and then, by ^{55}Fe ($T_{1/2}$ = 2.744 years).

Regarding the MgF_2 moderator, only ^{24}Na ($T_{1/2}$ = 14.997 h) is generated. A saturation C = 2 value is reached within 3 days of service, resulting in a cooling time of about 15 h. In the lead reflector, the activities of all radioactive products, as well as their normalized sum, remain well below the allowable levels.

3.3.4 ^{9}Be + p (30 MeV)

The C values and cooling times for the moderator and the reflector are shown in Figure 6, and for the fast neutron filters in Figure 7.

In the CaF_2 moderator, most of the activity is due to ^{18}F, which rapidly decays with a half-life of 109.77 min. The key contributors to the cooling time are initially ^{45}Ca ($T_{1/2}$ = 162.61 days), and later tritium ($T_{1/2}$ = 12.32 years) once it surpasses the clearance limit after 1 year of operation and ^{45}Ca had practically reached the saturation level. After approximately 15 years of service, ^{14}C (with a half-life of 5,700 years) reaches the clearance limit. Due to its longer half-life, the activity of ^{14}C becomes the primary factor defining the cooling time since then.

In a pure lead reflector, ^{203}Pb, with a half-life of 51.92 h, contributes significantly to C. However, the cooling time is primarily governed by ^{204}Tl ($T_{1/2}$ = 3.783 years) and tritium ($T_{1/2}$ = 12.32 years) once they exceed their respective clearance levels at approximately 1 month and 40 years of service, respectively.

Regarding the fast neutron filters, iron stands out as the most activated material, with C ranging from about 10^5 to 10^6 depending on the operation time. In pure iron, ^{55}Fe ($T_{1/2}$ = 2.744 years) rapidly surpasses the clearance limit (within the first day of operation), determining the cooling time until tritium ($T_{1/2=}$12.32 years) does so at 18 months of service.

The pure aluminum filter requires only 10–15 days of cooling when used for less than 6 months, mainly due to the presence of ^{24}Na ($T_{1/2}$ = 14.922 days) as the sole significant product. After approximately 4 months of operation, when ^{22}Na ($T_{1/2}$ = 2.6018 years) reaches its clearance level, cooling times increase to several years. Similarly, at around 9 months of operation, tritium reaches the clearance level, becoming the dominant factor in the cooling period, resulting in cooling times of several decades.

In the aluminum 1,050 alloy, ^{65}Zn ($T_{1/2}$ = 243.93 days) and ^{54}Mn ($T_{1/2}$ = 312.2 days) determine the cooling time during the first year of operation. Subsequently, tritium and ^{60}Co ($T_{1/2}$ = 1925.28 days), which have reached their clearance levels, become the relevant products in determining the cooling time.

Finally, in the pure lead filter, the most significant contribution comes from ^{203}Pb ($T_{1/2}$ = 51.92 h). Additionally, above the clearance level, there are ^{203}Hg ($T_{1/2}$ = 46.594 days), ^{202}Tl ($T_{1/2}$ = 12.31 days) ^{204}Tl and ($T_{1/2}$ = 3.783 years), with the latter having the most impact on the cooling time during early operation. Subsequently, after 8 months of operation, tritium reaches the clearance level and becomes the contributor that determines the cooling time.

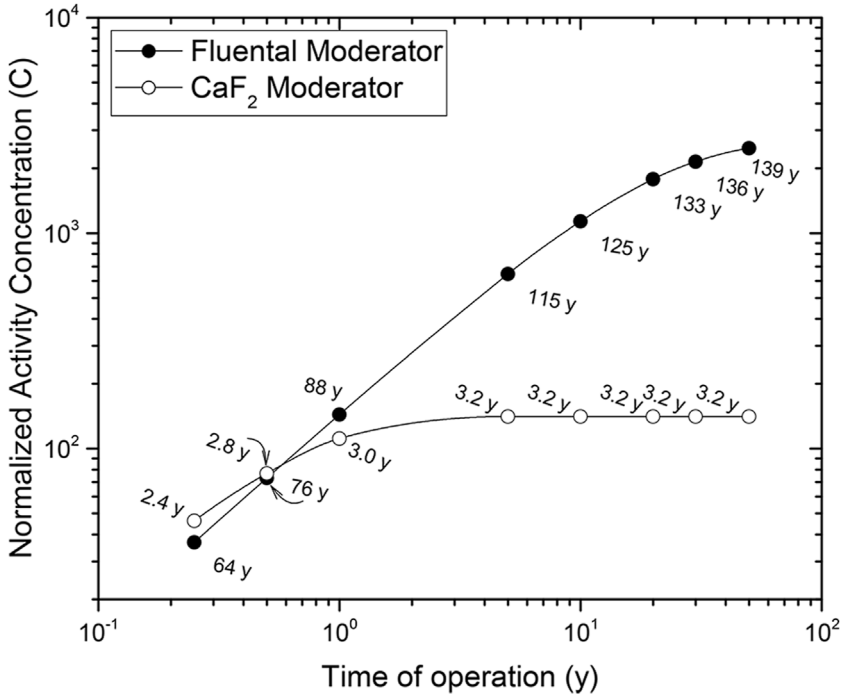

FIGURE 3
Normalized activity concentration (C) and cooling times for Fluental™ and CaF_2 moderators when employed with ^{7}Li targets and 30 mA of 2.3 MeV protons.

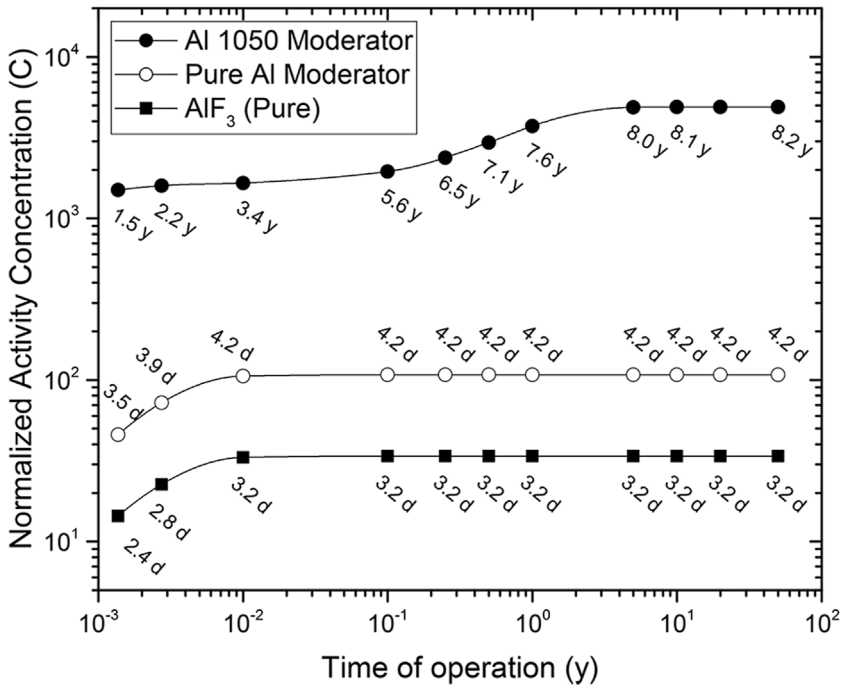

FIGURE 4
Normalized activity concentration (C) and cooling times for pure and alloyed (1,050) aluminum, as well as for AlF_3 moderators when employed with ^{9}Be and ^{13}C targets and a 30-mA beam of deuterons of 1.45 MeV.

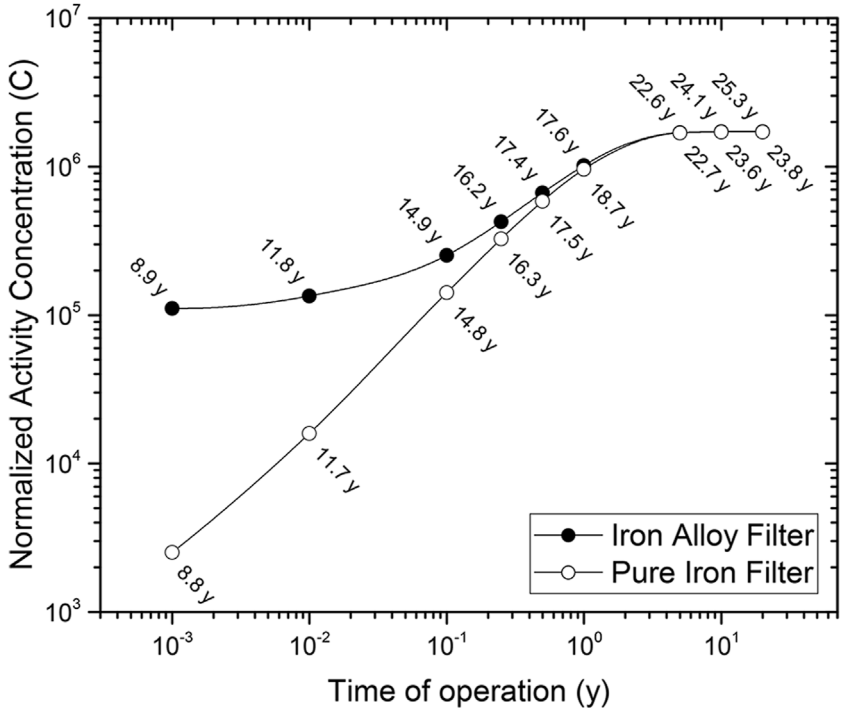

FIGURE 5
Normalized activity concentration (C) and cooling times for pure and alloyed iron when employed as a fast neutron filter with ^{9}Be targets and A 10-mA beam of 8 MeV protons.

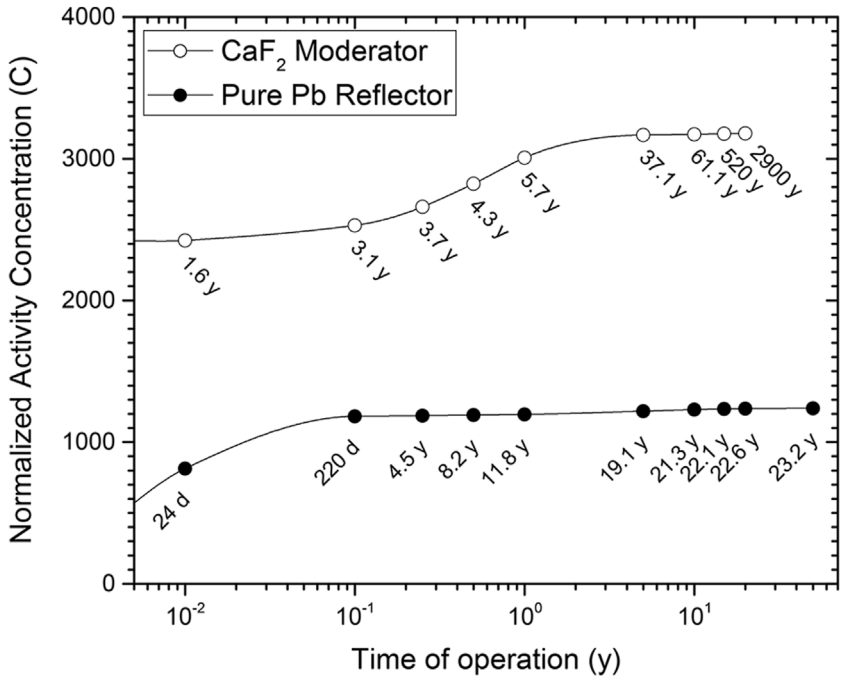

FIGURE 6
Normalized activity concentration (C) and cooling times for a CaF_2 moderator and a pure lead reflector when employed with ^{9}Be targets and a 1-mA beam of 30 MeV protons.

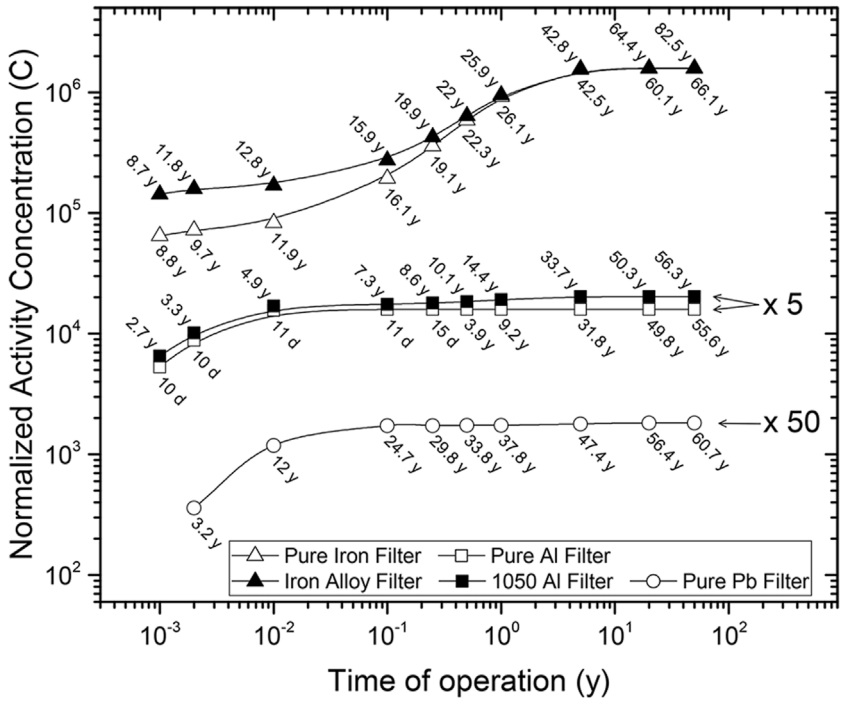

FIGURE 7
Normalized activity concentration (C) and cooling times for lead, aluminum, and iron as fast neutron filters with ^{9}Be targets and a 1-mA beam of 30 MeV protons.

TABLE 5 Radioactivity induced in targets and beam shaping assemblies for different AB-BNCT approaches.

		^{7}Li(p,n) 2.3 MeV, 30 mA	^{9}Be(p,n) 8 MeV, 10 mA	^{9}Be(p,n) 30 MeV, 1 mA	^{9}Be(d,n) 1.45 MeV, 30 mA	^{13}C(d,n) 1.45 MeV, 30 mA
Target: Radionuclides and activity after 30 days of operation		^{7}Be: 2.1TBq	Only prompt radiation	^{7}Be: 390 GBq ^{3}H: 4.2 GBq	^{3}H: 4.1 GBq	^{3}H: 780 MBq^{14}C: 2.2 kBq
BSA: Main radionuclides and cooling time after 5 years of operation	**Moderator**	Fluental: (^{3}H, 115 years)	MgF_2: None	CaF_2: (^{45}Ca, ^{3}H, 37.1 years)	PTFE + Al 1,050: (^{65}Zn,^{54}Mn, 8.0 years)	PTFE + Al 1,050: (^{65}Zn,^{54}Mn, 8.0 years)
		CaF_2: (^{45}Ca, 3.2 years)			AlF_3: None	AlF_3: None
		MgF_2: None				
		AlF_3: None				
	Reflector	Pb: None	Pb: None	Pb: (^{204}Tl, 19.1 years)	Pb: None	Pb: None
	Fast Neutron Filter		Iron: (^{54}Mn,^{55}Fe, 17.5 years)	Pb: (^{3}H,^{204}Tl, 47.4 years)		
				Al 1,050: (^{3}H,^{60}Co,^{65}Zn,^{54}Mn, 33.7 years)		
				Iron: (^{3}H,^{55}Fe,^{54}Mn, 42.8 years)		

4 Summary

Table 5 shows a comprehensive summary of the results obtained from the analyzed configurations for both the target and the BSA. The target activities are calculated for a 30-day period of operation, assuming a daily operation of 8 h. The cleanest target option is the ^{9}Be(p,n) case when using 8 MeV protons, since only prompt radiation is produced. Among the remaining options, the ^{13}C(d,n) case has the lowest activity.

As for the BSAs, the table shows information on the long-term activation of their elements (moderator, reflector, and fast neutron filters, when applicable) for all evaluated configurations. The information provided includes radionuclides that have the most significant impact on the cooling process, along with the corresponding cooling times. The cooling times corresponds to a 5-year operational period. Based on these results, long-term radioactivity can only be avoided in the BSA configuration ^{7}Li(p,n) when using MgF_2 or AlF_3 as a moderator, and in the cases of ^{9}Be(d,n) and ^{13}C(d,n) when using AlF_3 as a moderator.

5 Conclusion

A comprehensive evaluation was conducted on different targets and Beam Shaping Assemblies (BSAs) intended for Accelerator-Based Boron Neutron Capture Therapy (AB-BNCT). The primary focus of this assessment was to analyze their activation to facilitate a better understanding of the most suitable materials and configurations to effectively minimize the generation of residual radioactivity.

Regarding the targets, utilizing 8 MeV protons on a ^{9}Be target is the cleanest option: only prompt radiation and no radioactivity is generated. Conversely, the lithium target is the one with the highest activity, producing 2.1 TBq of ^{7}Be, a gamma-ray emitter with a half-life of 53.22 days, after 30 days of service. To minimize the gamma ray exposure (for instance, of workers involved in tasks such as handling or replacing the target) it is imperative to limit the target's service time to no more than a few days. The beryllium target, when bombarded with 30 MeV protons, also produces ^{7}Be, although at a lower level (390 GBq in 30 days) and generates tritium as well. Meanwhile, when 1.45 MeV deuterons are used with ^{9}Be and 13C targets, external exposure does not set a limitation, since only low-energy pure beta emitters are generated: tritium, in both targets and 14C in the 13C one. The kinetic energy of these beta particles is E < 18.591 keV and E < 156 keV for tritium and ^{14}C, respectively. Tritium's beta particles can be effectively stopped within less than 1 cm of air, and those from ^{14}C are halted in the outer protective dead layer of the skin. For these cases the limiting factor, instead of exposure, is the long-term activity accumulation, due to the half-lives of tritium and ^{14}C (12.32 years and 5,700 years, respectively).

In the BSA, activation is due to neutrons and the key factor to consider is their energy. Based on the neutron energy, AB-BNCT facilities can be classified as low (E < 1 MeV), intermediate (up to 6–8 MeV), and high (up to 28 MeV). Generally, higher neutron energies facilitate a greater number of energetically feasible reactions, leading to the generation of radioactive products.

The reactions leading to the most relevant radioactive product were identified for the common BSA materials and for each neutron energy group and based on the IAEA Safety Guide on Application of the Concepts of Exclusion, Exemption, and Clearance, the normalized activity concentrations and their respective cooling times were estimated over their lifespan, indicating which materials are most suitable for specific energy regimes. A detailed analysis was presented for some of the most common BSA materials.

In the low-energy group, only exothermic reactions produce radioactive products. For commonly used BSA materials, the dominant reaction type is (n,γ). Most of (n,p) (n,α) (n,d) are energetically forbidden, with the exception of materials containing ^{6}Li, where the exothermic (n,α) reaction yields tritium.

Fluental moderators are the potentially critical in this group, as they generate tritium activities that require decades of clearance. CaF_2 moderators demand about 3 years due to ^{45}Ca. Meanwhile, MgF_2 and AlF_3 moderators do not produce long-term radioactivity, making them the cleanest options as moderators.

In the intermediate-energy group most (n,p) (n,α) and (n,d) reactions become accessible for neutrons of these energies although the cross-sections are generally low in most BSA materials. However, there are exceptions in the cases of ^{27}Al(n,α)^{24}Na and ^{54}Fe(n,p)^{54}Mn, which result in radioactivity production in materials containing aluminum and iron, respectively. Tritium-producing reactions (n,t) are, in general, energetically forbidden for this group, as they have threshold energies ranging from about 8 to 10 MeV in most BSA materials.

The critical materials within this group are iron (whether pure or alloyed) and aluminum alloys. For iron, the main radionuclides that determine the clearance time are ^{56}Mn and ^{55}Fe, resulting in a clearance time of about 20 years. For aluminum alloys, it is imperative to consider the activation of the alloying components to estimate cooling times, as pure aluminum does not generate long-term radioactivity. Even for a high-content aluminum alloys like the 1,050 alloy, the cooling times may extend to several years. In their pure form, AlF_3 and MgF_2 stand out as the cleanest moderator options.

In the high-energy facilities, tritium producing reactions (n,t) reactions become accessible and significantly impact on the cooling time in some BSA materials including iron, aluminum and CaF_2. Reaction channels with multiple ejectiles (such as (n, 2n) (n,n + p) (n,n+α) etc.), which are forbidden at lower energies, become accessible and should be considered for total activity calculation.

After 5 years of operation, cooling times of approximately 30 years are necessary for pure aluminum, 40 years for CaF_2 and iron (whether alloyed or pure), and 50 years for lead when used as a fast neutron filter; whereas, when used as a reflector, nearly 20 years of cooling time are required. It was observed that to control and limit cooling times, it is crucial to ensure that the longest-lived radionuclide generated in each material remains below its respective clearance level.

Data availability statement

The raw data supporting the conclusion of this article will be made available by the authors, without undue reservation.

Author contributions

MC: Formal Analysis, Investigation, Methodology, Visualization, Writing–original draft, Data curation, Resources, Software, Validation. AK: Conceptualization, Methodology, Project administration, Resources, Supervision, Writing–review and editing, Funding acquisition.

Funding

The author(s) declare financial support was received for the research, authorship, and/or publication of this article. This work

was supported by the National Atomic Energy Commission (CNEA), Argentina.

Conflict of interest

The authors declare that the research was conducted in the absence of any commercial or financial relationships that could be construed as a potential conflict of interest.

Publisher's note

All claims expressed in this article are solely those of the authors and do not necessarily represent those of their affiliated organizations, or those of the publisher, the editors and the reviewers. Any product that may be evaluated in this article, or claim that may be made by its manufacturer, is not guaranteed or endorsed by the publisher.

References

Aleynik, V., Burdakov, A., Davydenko, V., Ivanov, A., Kanygin, V., Kuznetsov, A., et al. (2011). BINP accelerator based epithermal neutron source. *Appl. Radiat. Isot.* 69, 1635–1638. doi:10.1016/j.apradiso.2011.03.010

Bae, Y., Kim, D.-S., Seo, H. J., Han, J.-U., Yoon, H. J., Hwang, J. J., et al. (2022). Advances of LINAC-based boron neutron capture therapy in Korea. *AAPPS Bull.* 32, 34. doi:10.1007/s43673-022-00063-2

Brown, D. A., Chadwick, M. B., Capote, R., Kahler, A. C., Trkov, A., Herman, M. W., et al. (2018). ENDF/B-VIII.0: the 8th major release of the nuclear reaction data library with CIELO-project cross sections, new standards and thermal scattering data. *Nucl. Data Sheets* 148, 1–142. doi:10.1016/j.nds.2018.02.001

Capoulat, M. E. (2014a). Estudio de la reacción ^{9}Be(d,n)^{10}B como fuente de neutrones para la Terapia por Captura Neutrónica en Boro (BNCT) PhD Thesis. Available at: https://www.cnea.gob.ar/nuclea/handle/10665/1837.

Capoulat, M. E., and Kreiner, A. J. (2017). A ^{13}C(d,n)-based epithermal neutron source for Boron Neutron Capture Therapy. *Phys. Medica* 33, 106–113. doi:10.1016/j.ejmp.2016.12.017

Capoulat, M. E., and Kreiner, A. J. (2022). "Review of the different accelerator-based BNCT facilities worlwide and an assessment according to the alara criterion," in *International conference on accelerators for research and sustainable development, conference materials Vol.3 – full papers*, 248–260.

Capoulat, M. E., Minsky, D. M., and Kreiner, A. J. (2014b). Computational assessment of deep-seated tumor treatment capability of the ^{9}Be(d,n)^{10}B reaction for accelerator-based Boron Neutron Capture Therapy (AB-BNCT). *Phys. Medica* 30, 133–146. doi:10.1016/j.ejmp.2013.07.001

Cartelli, D. E., Capoulat, M. E., Baldo, M., Sandín, J. C. S., Igarzabal, M., Grosso, M. F. D., et al. (2020). Status of low-energy accelerator-based BNCT worldwide and in Argentina. *Appl. Radiat. Isot.* 166, 109315. doi:10.1016/j.apradiso.2020.109315

Chen, J., Hu, Z., Tong, J., Zhou, B., Zhang, R., Zhao, C., et al. (2021). Study of BNCT neutronics optimization for out-of-beam dosimetry based on radiobiological figures of merit. *Nucl. Instrum. Methods Phys. Res. Sect. B Beam Interact. Mater. Atoms* 508, 1–9. doi:10.1016/j.nimb.2021.09.014

Chen, J.-Y., Tong, J.-F., Hu, Z.-L., Han, X.-F., Tang, B., Yu, Q., et al. (2022). Evaluation of neutron beam characteristics for D-BNCT01 facility. *Nucl. Sci. Tech.* 33, 12. doi:10.1007/s41365-022-00996-1

Goorley, T., James, M., Booth, T., Brown, F., Bull, J., Cox, L. J., et al. (2012). Initial MCNP6 release overview. *Nucl. Technol.* 180, 298–315. doi:10.13182/NT11-135

Halfon, S., Arenshtam, A., Kijel, D., Paul, M., Weissman, L., Berkovits, D., et al. (2015). Demonstration of a high-intensity neutron source based on a liquid-lithium target for Accelerator based Boron Neutron Capture Therapy. *Appl. Radiat. Isot.* 106, 57–62. doi:10.1016/j.apradiso.2015.07.045

Hermanne, A., Tarkanyi, F., and Takacs, S. (2014). Activation cross sections for production of 7Be by proton and deuteron induced reactions on 9Be: protons up to 65MeV and deuterons up to 50MeV. *Appl. Radiat. Isot.* 90, 203–207. doi:10.1016/j.apradiso.2014.04.005

International Atomic Energy Agency (2004). *Application of the Concepts of exclusion, exemption and clearance, safety standard serires Nº RS-G-1.7*. Vienna: International Atomic Energy Agency.

International Atomic Energy Agency (2005). *Derivation of activity concentration values for exclusion, exemption and clearance, safety report series Nº 44*. Vienna: International Atomic Energy Agency.

International Atomic Energy Agency (2022). *Advances in Boron neutron capture Therapy*. Vienna: International Atomic Energy Agency.

Kansai Bnct Medical Center, (2019). Kansai BNCT medical center. Available at: https://www.ompu.ac.jp/kbmc/en.html (Accessed May 12, 2022).

Kato, T., Hirose, K., Tanaka, H., Mitsumoto, T., Motoyanagi, T., Arai, K., et al. (2020). Design and construction of an accelerator-based boron neutron capture therapy (AB-BNCT) facility with multiple treatment rooms at the Southern Tohoku BNCT Research Center. *Appl. Radiat. Isot.* 156, 108961. doi:10.1016/j.apradiso.2019.108961

Komori, S., Hirose, K., Takeuchi, A., Kato, R., Motoyanagi, T., Yamazaki, Y., et al. (2023). Characterization and clinical utility of different collimator shapes in accelerator-based BNCT systems for head and neck cancer. *Phys. Medica* 112, 102625. doi:10.1016/j.ejmp.2023.102625

Koning, A. J., Rochman, D., Sublet, J. C., Dzysiuk, N., Fleming, M., and van der Marck, S. (2019). TENDL: complete nuclear data library for innovative nuclear science and technology. *Nucl. Data Sheets* 155, 1–55. doi:10.1016/j.nds.2019.01.002

Kreiner, A. J., Kwan, J. W., Burlón, A. A., Di Paolo, H., Henestroza, E., Minsky, D. M., et al. (2007). A Tandem-electrostatic-quadrupole for accelerator-based BNCT. *Nucl. Instrum. Methods Phys. Res. Sect. B Beam Interact. Mater. Atoms* 261, 751–754. doi:10.1016/j.nimb.2007.04.055

Kumada, H., Kurihara, T., Yoshioka, M., Kobayashi, H., Matsumoto, H., Sugano, T., et al. (2015). Development of beryllium-based neutron target system with three-layer structure for accelerator-based neutron source for boron neutron capture therapy. *Appl. Radiat. Isot.* 106, 78–83. doi:10.1016/j.apradiso.2015.07.033

Kumada, H., Matsumura, A., Sakurai, H., Sakae, T., Yoshioka, M., Kobayashi, H., et al. (2014). Project for the development of the linac based NCT facility in University of Tsukuba. *Appl. Radiat. Isot.* 88, 211–215. doi:10.1016/j.apradiso.2014.02.018

Kumada, H., Naito, F., Hasegawa, K., Kobayashi, H., Kurihara, T., Takada, K., et al. (2018). Development of LINAC-based neutron source for boron neutron capture therapy in university of tsukuba. *Plasma Fusion Res.* 13, 2406006. doi:10.1585/pfr.13.2406006

Kumada, H., Takada, K., Naito, F., Kurihara, T., Sugimura, T., Matsumoto, Y., et al. (2019). "Beam performance of the iBNCT as a compact linac-based BNCT neutron source developed by University of tsukuba," in *AIP conference proceedings (American Institute of Physics inc)* 050013. doi:10.1063/1.5127705

Lee, C. H., Moon, M., Lee, D. W., Kim, H. S., Kwon, H. J., Lee, P., et al. (2021a). Status of development and planning activities on CANS in Korea. *J. Neutron Res.* 23, 127–141. doi:10.3233/JNR-210017

Lee, P. Y., Tang, X., Geng, C., and Liu, Y. H. (2021b). A bi-tapered and air-gapped beam shaping assembly used for AB-BNCT. *Appl. Radiat. Isot.* 167, 109392. doi:10.1016/j.apradiso.2020.109392

Li, G., Jiang, W., Zhang, L., Chen, W., and Li, Q. (2021). Design of beam shaping assemblies for accelerator-based BNCT with multi-terminals. *Front. Public Heal.* 9, 642561. doi:10.3389/fpubh.2021.642561

Matsumura, A., Asano, T., Hirose, K., Igaki, H., Kawabata, S., and Kumada, H. (2023). Initiatives toward clinical boron neutron capture therapy in Japan. *Cancer biother. Radiopharm.* 38, 201–207. doi:10.1089/cbr.2022.0056

Mitsumoto, T. (2023). "Proton cyclotron accelerator and beryllium target system," in *Advances in accelerators and medical Physics* (Amsterdam, Netherlands: Elsevier), 225–233. doi:10.1016/b978-0-323-99191-9.00023-2

Mitsumoto, T., Yajima, S., Tsutsui, H., Ogasawara, T., Fujita, K., Tanaka, H., et al. (2013). "Cyclotron-based neutron source for BNCT," in *AIP conference proceedings (AIP publishing)*, 319–322. doi:10.1063/1.4802341

Nakamura, S., Igaki, H., Ito, M., Imamichi, S., Kashihara, T., Okamoto, H., et al. (2021). Neutron flux evaluation model provided in the accelerator-based boron neutron capture therapy system employing a solid-state lithium target. *Sci. Rep.* 11, 8090–8113. doi:10.1038/s41598-021-87627-8

Nakayama, S., Iwamoto, O., Watanabe, Y., and Ogata, K. (2021). JENDL/DEU-2020: deuteron nuclear data library for design studies of accelerator-based neutron sources. *J. Nucl. Sci. Technol.* 58, 805–821. doi:10.1080/00223131.2020.1870010

National Nuclear Data Center (2022). NuDat database. Available at: https://www.nndc.bnl.gov/nudat3/(Accessed May 20, 2022).

NEUBORON (2021). Boron neutron capture therapy. Available at: https://en.neuboron.com/bnct (Accessed September 14, 2023).

Neutron Therapeutics Inc (2019a). Neutron therapeutics installs europe's first accelerator-based boron neutron capture therapy (BNCT) platform. Available at: https://www.neutrontherapeutics.com/news/pr-041819/(Accessed May 12, 2022).

Neutron Therapeutics Inc (2019b). Technology – neutron therapeutics. Available at: https://www.neutrontherapeutics.com/technology/(Accessed September 14, 2023).

Neutron Therapeutics Inc (2023). Neutron therapeutics announces successful generation of a neutron beam for BNCT at shonan kamakura general hospital in Japan | business wire. Available at: https://www.businesswire.com/news/home/20230112005081/en/Neutron-Therapeutics-Announces-Successful-Generation-of-a-Neutron-Beam-for-BNCT-at-Shonan-Kamakura-General-Hospital-in-Japan (Accessed September 14, 2023).

Porra, L., Seppälä, T., Wendland, L., Revitzer, H., Joensuu, H., Eide, P., et al. (2022). Accelerator-based boron neutron capture therapy facility at the Helsinki University Hospital. *Acta Oncol. Madr.* 61, 269–273. doi:10.1080/0284186X.2021.1979646

Porras, I., Praena, J., Arias de Saavedra, F., Pedrosa-Rivera, M., Torres-Sánchez, P., Sabariego, M. P., et al. (2020). BNCT research activities at the Granada group and the project NeMeSis: neutrons for medicine and sciences, towards an accelerator-based facility for new BNCT therapies, medical isotope production and other scientific neutron applications. *Appl. Radiat. Isot.* 165, 109247. doi:10.1016/j.apradiso.2020.109247

Qiao, Z., Ma, B., Rong, B., Jiang, Q., and Wang, S. (2023). Beam shaping assembly design of Li(p,n) neutron source with a rotating target for boron neutron capture therapy. *Nucl. Instrum. Methods Phys. Res. Sect. A Accel. Spectrom. Detect. Assoc. Equip.* 1052, 168249. doi:10.1016/j.nima.2023.168249

Southern Tohoku Hospital Group (2020). Southern TOHOKU BNCT research center. Available at: http://www.sthg-jp.com/motion.asp?siteid=100511&menuid=10491&lgid=1 (Accessed May 12, 2022).

Sublet, J.-C., Packer, L. W., Kopecky, J., Forrest, R. A., Koning, A. J., and Rochman, D. A. (2010). *The European Activation File: EAF-2010 neutron-induced cross section library*.

Suzuki, S., Nitta, K., Yagihashi, T., Eide, P., Koivunoro, H., Sato, N., et al. (2023). Initial evaluation of accelerator-based neutron source system at the Shonan Kamakura General Hospital. *Appl. Radiat. Isot.* 199, 110898. doi:10.1016/j.apradiso.2023.110898

TAE Life Sciences (2021). Alphabeam™ system. Available at: https://taelifesciences.com/alphabeam-neutron-system/(Accessed September 14, 2023).

Tanaka, H., Sakurai, Y., Suzuki, M., Masunaga, S., Kinashi, Y., Kashino, G., et al. (2009). Characteristics comparison between a cyclotron-based neutron source and KUR-HWNIF for boron neutron capture therapy. *Nucl. Instrum. Methods Phys. Res. Sect. B Beam Interact. Mater. Atoms* 267, 1970–1977. doi:10.1016/j.nimb.2009.03.095

Tanaka, H., Sakurai, Y., Suzuki, M., Masunaga, S., Mitsumoto, T., Fujita, K., et al. (2011). Experimental verification of beam characteristics for cyclotron-based epithermal neutron source (C-BENS). *Appl. Radiat. Isot.* 69, 1642–1645. doi:10.1016/j.apradiso.2011.03.020

Torres-Sánchez, P., Porras, I., Ramos-Chernenko, N., Arias de Saavedra, F., and Praena, J. (2021). Optimized beam shaping assembly for a 2.1-MeV proton-accelerator-based neutron source for boron neutron capture therapy. *Sci. Rep.* 11, 7576–7612. doi:10.1038/s41598-021-87305-9

University of Birmingham (2022). High-flux neutron facility launched at the university of birmingham - university of birmingham. Available at: https://www.birmingham.ac.uk/news/2022/high-flux-neutron-facility-launched-at-the-university-of-birmingham (Accessed September 14, 2023).

Uritani, A., Menjo, Y., Watanabe, K., Yamazaki, A., Kiyanagi, Y., and Tsuchida, K. (2018). *Design of beam shaping assembly for an accelerator-driven BNCT system*. Nagoya: Nagoya University Physical Society of Japan. doi:10.7566/jpscp.22.011002

Wang, Y., Wang, Z., Li, N., Guan, X., and Gu, L. (2022). Design of beam shaping assembly for accelerator-based boron neutron capture therapy and study on its clinical parameter. *Yuanzineng Kexue Jishu/Atomic Energy Sci. Technol.* 56, 1440–1447. doi:10.7538/yzk.2021.youxian.0467

Watanabe, K., Yoshihashi, S., Ishikawa, A., Honda, S., Yamazaki, A., Tsurita, Y., et al. (2021). First experimental verification of the neutron field of Nagoya University Accelerator-driven neutron source for boron neutron capture therapy. *Appl. Radiat. Isot.* 168, 109553. doi:10.1016/j.apradiso.2020.109553

Ziegler, J. F., Ziegler, M. D., and Biersack, J. P. (2010). SRIM - the stopping and range of ions in matter (2010). *Nucl. Instrum. Methods Phys. Res. Sect. B Beam Interact. Mater. Atoms* 268, 1818–1823. doi:10.1016/j.nimb.2010.02.091